Alleviating the barrier of adventitious roots formation in recalcitrant mature tissue by slow release of a synthetic auxin

Ohad Roth[1], Sela Yechezkel[2], Ori Serero[2,3], Avi Eliyahu[2,3], Inna Vints[1], Pan Tzeela[2,3], Alberto Carignano[4], Dorina P. Janacek[5], Verena Peters[6], Amit Kessel[7], Vikas Dwivedi[2], Mira Carmeli-Weissberg[2], Felix Shaya[2], Adi Faigenboim-Doron[2], Kien Lam Ung[8], Bjørn Panyella Pedersen[8], Joseph Riov[3], Eric Klavins[4], Corinna Dawid[6], Ulrich Z. Hammes[5], Nir Ben-Tal[7], Richard Napier[9], Einat Sadot[2*], Roy Weinstain[1*]

[1] School of Plant Sciences and Food Security, Faculty of Life Sciences, Tel Aviv University, Tel Aviv, Israel

[2] The Institute of Plant Sciences, The Volcani Center, Ministry of Agriculture and Rural Development, Israel

[3] The Robert H. Smith Institute of Plant Sciences and Genetics in Agriculture, The Robert H. Smith Faculty of Agriculture, Food and Environment, The Hebrew University of Jerusalem, Rehovot, Israel

[4] Department of Electrical and Computer Engineering, University of Washington, Seattle, United States

[5] Chair of Plant Systems Biology, Technical University of Munich, Freising, Germany

[6] Chair of Food Chemistry and Molecular and Sensory Science, Technical University of Munich, Freising, Germany

[7] Department of Biochemistry and Molecular Biology, School of Neurobiology, Biochemistry & Biophysics, Faculty of Life Sciences, Tel Aviv University, Tel Aviv, Israel

[8] Department of Molecular Biology and Genetics, Aarhus University, Aarhus, Denmark

[9] School of Life Sciences, University of Warwick, Coventry, UK

***** Correspondence should be addressed to E.S. (email: vhesadot@volcani.agri.gov.il) or to R.W. (email: royweinstain@tauex.tau.ac.il)

Abstract

Clonal propagation of plants by induction of adventitious roots (ARs) from stem cuttings is a requisite step in breeding programs. Nevertheless, a major barrier exists for propagating valuable plants that naturally have low capacity to form ARs. Due to the central role of auxin in organogenesis, indole-3-butyric acid (IBA) is often utilized, yet many recalcitrant plants do not form ARs in response to such treatment. We describe the synthesis and screening of a focused library of synthetic auxin conjugates in *Eucalyptus grandis* cuttings, highlighting 4-chlorophenoxyacetic acid-L-tryptophan-OMe as a competent enhancer of adventitious rooting in a number of recalcitrant woody plants. Comprehensive metabolic and functional analyses revealed that this activity is engendered by prolonged auxin signaling due to initial fast uptake and slow release and clearance of the free auxin 4-chlorophenoxyacetic acid. This work highlights the utility

of a slow-release strategy for bioactive compounds and provides an exemplar for further rational development of more effective plant-growth regulators for agriculture.

Introduction

Adventitious roots (ARs) are defined as roots that regenerate from non-root tissues, in contrast to lateral roots (LR) that are post-embryonic roots formed from root tissue[1]. Clonal (vegetative) propagation of plants by induction of ARs from stem cuttings is a requisite step in selection and breeding programs as well as in routine agricultural practices and has tremendous economic importance[2]. Clonal propagation is also a cornerstone in forestry, the ornamental plant industry, and the development of elite rootstocks to provide resistance to pests, diseases and changing environmental conditions[2]. Despite its significant economic and agricultural importance, a major barrier still exists for propagating clones of many valuable plants that naturally have low capacity (and often, none) to form ARs or that lose this ability during maturation[3–5].

AR development is a heritable, quantitative genetic trait[6,7] that shows high plasticity and is controlled by multiple intrinsic and environmental factors[8–10]. In particular, it was shown to be controlled by a complex network of plant hormones crosstalk, in which auxin signaling plays a central role in each step of the process[11–15]. In some plant species, lower endogenous indole 3-acetic acid (IAA) levels in difficult-to-root mature cuttings compared to easy-to-root juvenile ones, e.g., *Eucalyptus grandis* (*E. grandis*) and *Pisum sativum (P. sativum*), have been reported[16,17], as well as absence of IAA maxima in the cambium zone of difficult-to-root pine cuttings[18]; the cambium being the tissue from which ARs typically form[19] and where IAA maxima are often observed[20,21]. However, other plant species show comparable endogenous auxin levels in juvenile and mature shoots or even higher in the mature difficult-to-root ones[22,23] yet the ability to form AR is significantly impaired in mature shoots, with or without exogenous auxin application. Thus, the accepted presumption to date is that auxin responsiveness (as derived from auxin metabolism, transport and perception) has changed in mature cuttings, not any more able to convey the correct signaling pathways to support AR formation. Indeed, stronger auxin response (*DR5:GUS*) was reported in young vs. mature cuttings of *P. sativum* upon similar exogenous auxin treatments[16] and differential expression profiles of auxin-regulated genes were observed in easy- vs. difficult-to-root poplar[24,25], pine[18,26,27] and *Eucalyptus* species[17,28–31] along AR induction.

Although IAA is the most prevalent endogenous auxin in plants, and the first to be used for induction of AR formation[32], indole 3-butyric acid (IBA) and 1-naphthalaneacetic acid (NAA) have been found to be more efficient and for the past 60 years are the major components in most commercial rooting formulas[2,33]. Initially, the increased efficacy of IBA and NAA was attributed to

their higher light-resistance, but more recent studies point to their differential metabolism and transport (compared to IAA) as the potential source for their efficacy[34–36]. Over the years, efforts have been made to increase the effectiveness of IBA by different approaches, including its conjugation to various molecules[37–40]. Nevertheless, many recalcitrant plants respond poorly to exogenous application of these compounds[41,42], and their vegetative propagation remains a significant challenge.

The above observations have prompted us to hypothesize that synthetic auxins might represent an underexplored chemical space of bioactive compounds that could assist in overcoming the loss of rooting capability in difficult-to-root plants. Synthetic auxins constitute a large set of small organic molecules with structural resemblance to IAA and that mimic the effects of the endogenous IAA by promoting the interaction between the auxin receptors TRANSPORT INHIBITOR RESPONSE1 (TIR1)/AUXIN-SIGNALING F-BOX (AFB) and Aux/IAA[43]. Despite this central similarity, differences in metabolism[44], transport[45,46] and perception specificity[47–49] have been observed between IAA and several synthetic auxins (and among themselves), that presumably lead to different expression profiles of auxin responsive genes and/or sets of auxin-related phenotypes[49,50]. A number of synthetic auxins have been previously shown to promote rooting[51] (e.g. 2,4-dichlorophenoxyacetic acid (2,4-D) and 2,4,5-trichlorophenoxyacetic acid (2,4,5-T), however, with the exception of NAA, their high auxin activity limits their practical use due to high phytotoxicity, or promotion of callus instead of roots[52]. We envisioned that the inherent phytotoxicity and growth-inhibitory effect of synthetic auxins could be mitigated by their slow release *in planta*, maintaining a low yet functional level of the bioactive molecule over a prolonged time, thus opening the door to utilizations beyond their traditional role as herbicides[53]. Moreover, lengthy auxin treatments were reported to improve AR induction[54–57], which could further enhance the effectiveness of a slow-release approach.

To test this hypothesis, we synthesized a rationally-designed, focused library of four synthetic auxins conjugated to different residues, under the presumption that the conjugates will be hydrolyzed *in planta* (either enzymatically or chemically) to release the parent synthetic auxin. The conjugates were evaluated on difficult-to-root cuttings obtained from mature parts of *E. grandis* trees (Fig. 1a). A leading compound was found to enhance basal regeneration rates by 2-3-fold when applied to cuttings from diverse woody species. The dynamics underlying the compound activity is described herein.

Results

Design, synthesis, and screening of synthetic auxins conjugates

To develop a suitable chemical library, the synthetic auxins 4-chlorophenoxyacetic acid (4-CPA) (**1**), 2-methyl-4-chlorophenoxyacetic acid (MCPA) (**2**), 2-(2,4-dichlorophenoxy) propionic acid (2-DP) (**3**), and NAA (**4**) were chosen for conjugation. The first three belong to the phenoxy acid family[58] and feature a relatively strong, medium, and weak auxin activity, respectively, as determined by root elongation inhibition of *Prosopis juliflora*[59]. NAA belongs to the aromatic acetate family[60] and is often used in commercial rooting enhancement mixtures[2]. Each of the synthetic auxins (**1**–**4**) was conjugated through its carboxylic acid, a required moiety for the hormone biological activity[61–63], with a series of amine residues or methanol, forming a set of 39 conjugates (**1**–**4a**–**q,** Supplementary Fig. 1). The rooting enhancement capability of the conjugates and the free auxins (43 compounds in total) was evaluated using cuttings from mature *E. grandis* trees, which regenerate roots at low efficiency following 1 min submergence treatment with K-IBA, the potassium salt of IBA and the agricultural "gold standard" rooting enhancer[6]. The conjugates (100 M) were applied by submerging the cutting base for 1 min or by spraying the cutting apical part, either as a standalone treatment or in combination with a 6,000 ppm K-IBA (24.9 mM) submergence treatment. The cuttings were then incubated in a rooting table for approximately 1 month before examination. In total, 20–90 cuttings were tested per conjugate-based treatment and ~500 cuttings per K-IBA control treatment. At the chosen screening concentration (100 M), none of the compounds outperformed K-IBA as a standalone treatment, however applications based on the combination of compounds **1a**, **1j**, **1o**, **1p** or **1q** with K-IBA showed significantly higher rooting rates (Supplementary Fig. 2). Of these compounds, **1q**, a conjugate of 4-CPA to L-tryptophan methyl ester (L-Trp-OMe, Fig. 1b), had the strongest effect, with nearly 40% root regeneration for either spray or submergence treatments when combined with K-IBA, compared to 17% for K-IBA alone (Supplementary Fig. 2). Of note, the corresponding free synthetic auxins at a similar concentration had no positive effect when combined with K-IBA. Likewise, increasing the amount of K-IBA applied as a single treatment from 6,000 up to 12,000 ppm did not improve rooting rates (Supplementary Fig. 3), and HPLC-MS/MS analysis shows similar IBA levels in cuttings 15 min after application of K-IBA or K-IBA+**1q** (Supplementary Fig. 4), ruling out mere increase in auxin levels or IBA uptake as underlying the effect observed when conjugates were added. Due to its hydrophobicity, applying higher concentrations of **1q** in a water-based solution was found to be challenging. As an alternative, we combined spray and submergence treatments, each at three different concentrations (20, 50 and 100 M), in addition to 6,000 ppm K-IBA, in order to increase

the applied concentration of **1q**. Strikingly, this dual application method resulted in AR induction efficiencies of 66% and 77% in response to **1q** at 20 and 50 M, respectively (Fig. 1c), ~3-folds higher than K-IBA alone. This effect was accompanied by the formation of comparable number, however significantly longer, roots per rooted cutting compared to K-IBA (Fig. 1d,e). To conclude, we find that a simple and short application of a synthetic auxin-based conjugate significantly augmented the saturated effect of K-IBA on de-novo root regeneration, which is a critical practice for the agricultural industry.

Distinct bioavailability of 4-CPA underlies the activity of 1q

We speculated that **1q** exerts its bioactivity via a two-step process, in which **1q** is first hydrolyzed to its carboxylic acid form (**1r**), followed by removal of the amino acid that leads to release of bioactive 4-CPA (Fig. 2a). To rule out the possibility that **1q** itself can interact with the auxin perception machinery, and thus directly modulate AR formation, its ability to affect the TIR1-Aux/IAA7 auxin-perception complex formation was evaluated *in vitro* via surface plasmon resonance (SPR) measurements. The results show that neither **1q** nor **1r** have any measurable auxin or anti-auxin activity (Fig. 2b and Supplementary Fig. 5, respectively). Thus, the activity of **1q** seems to depend on its ability to release a bioactive 4-CPA. To understand the fate of **1q** *in planta*, cuttings of *E. grandis* were submerged and sprayed with either 4-CPA or **1q** (in addition to K-IBA submergence), and the small-molecules content of the cutting bases were analyzed periodically via HPLC-MS/MS for up to 8 days following treatment. Figure 2c shows the metabolic derivatives of **1q** following its application, and Figure 2d shows the levels of 4-CPA measured following **1q** or free 4-CPA application. The first time point, 1 h post-application, illuminates one of the features of **1q**; the esterification of the carboxylic acid leads to a more hydrophobic molecule (logD at pH = 7.0: 0.06 vs. 3.17), resulting in a 10-fold higher uptake of **1q** (Fig 2c) compared to free 4-CPA (Fig. 2d) (515.5 ± 24.4 vs. 53.2 ± 5.6 pg/mg fresh weight (FW)). This time point also demonstrates the rapid de-esterification of **1q** *in planta*, with ~13% **1r** out of the measured **1q**-derived forms, and a negligible amount of 4-CPA, pointing to the amide bond cleavage as the rate-limiting step in 4-CPA release. Indeed, 6 h after application, **1q** levels decreased by ~82% (to 90.9 ± 4.1 pg/mg FW) while comparable **1r** and 4-CPA levels were detected (48.5 ± 0.8 and 38.2 ± 1.1 pg/mg FW, respectively). This observation suggests that initially, a significant portion of **1q** is not available for immediate de-esterification. In the subsequent ~48 h, **1q** level remained relatively constant whilst a clear conversion of **1r** to 4-CPA was detected. Interestingly, despite the higher uptake of **1q** compared to free 4-CPA, the maximal level of 4-CPA was comparable in both treatments (53.2 ± 4.0 and 72.0 ±

2.0 pg/mg FW for 4-CPA or **1q**, respectively) (Fig. 2d). However, the timing of their formation was strikingly different; while 4-CPA level peaked 1 h post-application for the free 4-CPA (Fig. 2d), it only peaked after 24 h for **1q** (Fig. 2c). In addition, clearance rates were very different; 4-CPA retained an approximate physiologically relevant level of an auxin (>10 pg/mg FW, as measured for IAA in *E. grandis* cuttings, Supplementary Fig. 6) for only 2 days when applied directly but persisted for >6 days when applied in the form of **1q** (Fig. 2c,d). The above observations suggest that **1q** application could support prolonged auxin signaling *in planta*. To further evaluate this point, we turned to *Arabidopsis thaliana* (*Arabidopsis*), first seeking to establish the activity of **1q** in this model plant and then to correlate it with auxin signaling. In line with the results in *E. grandis*, a brief (1.5 h) shoot application of **1q**, but not of 4-CPA or IBA (10 M), resulted in a substantial increase in AR formation of intact etiolated *Arabidopsis* seedlings (Fig. 2e, Supplementary Fig. 7). In accord, applying the same treatment to *Arabidopsis DR5:Luciferase* line, encoding for a high turnover auxin reporter suitable for long-term imaging[64], led to stronger and more prolonged auxin signaling in response to **1q** compared to 4-CPA (Fig. 2f). Importantly, these observations also demonstrate that K-IBA treatment is not necessarily a prerequisite for the activity of **1q**. Collectively, the results of the above experiments suggest that **1q** serves as a reservoir for continuous auxin release that promotes AR induction and development.

Weak receptor-binding and altered cellular stability and mobility shape 4-CPA activity

In addition to the characteristics of the conjugate, which engender higher uptake and slow auxin release, intrinsic properties of the released synthetic auxin might shape the cellular responses to **1q** and were therefore examined. SPR measurements showed that 4-CPA is a ~2-orders of magnitude weaker binder of TIR1 than IAA (Fig. 2b). A comparable weaker auxin activity was found *in vivo*, using qualitative (lacZ-based, TIR1+Aux/IAA7, Supplementary Fig. 8a) and quantitative (degron-YFP based, TIR1+Aux/IAA9 and AFB2+Aux/IAA9) yeast-2-hybrid (Y2H) assays (Supplementary Fig. 8b). Initial weak auxin activity was also found in root growth inhibition and *DR5:Venus* response assays in *Arabidopsis* (Fig. 3a,b). Several synthetic auxins were shown to evoke unique expression profiles of auxin responsive genes compared to IAA[50], which could underlie the AR promotion activity observed for **1q**. An extended analysis of 4-CPA binding performances by a systematic evaluation of 11 Aux/IAA and both TIR1 and AFB2 receptors (with the appropriate EC_{50} for each, calculated from the curves shown in Supplementary Fig. 8b), did not reveal a specific degradation pattern in response to 4-CPA (Fig. 3c and Supplementary Fig. 8c). Thus, based on the *Arabidopsis* auxin perception mechanism, a differential signaling response to 4-CPA as a

result of unique binding is unlikely. Nevertheless, while *Arabidopsis* root growth recovers quickly from IAA inhibition, it is entirely arrested in response to 4-CPA (Fig. 3a), suggesting differences in transport and/or catabolism between the two molecules. A shoot-to-root movement assay in *Arabidopsis* implied that 4-CPA is a mobile auxin (Supplementary Fig. 9). However, although 4-CPA was found to utilize the native IAA importer AUXIN-RESISTANT1 (AUX1) (Fig. 3d,e), a solid-supported membrane (SSP)-based electrophysiology assay testing the transport activity of PIN-FORMED8 (PIN8), an adopted model for PINs activity[65], demonstrated that unlike IAA (and the analogue 2,4-D[65]), 4-CPA did not induce a significant current response at the concentration tested (20 M) (Fig. 3f). These observations suggest that 4-CPA is only partially subjected to the canonical polar auxin transport mechanism. Unlike 4-CPA, AUX1-expressing oocytes did not accumulate **1r** upon 30 min incubation (Supplementary Fig. 10a), and comparable levels of **1q** (and its derivative **1r**) were found in both AUX1-expressing and non-expressing oocytes (Supplementary Fig. 10b). To evaluate the contribution of 4-CPA movement to AR formation following **1q** treatment, we examined the *aux/lax* quadruple mutant[66], and found it insensitive to AR induction by **1q** (brief shoot application, Supplementary Fig. 11). Together, these experiments suggest that cell-to-cell movement of 4-CPA, but not of its precursors, is crucial for effective AR induction in response to a brief treatment of **1q**. To address the hypothesis that 4-CPA differs from IAA not only in transport but also in catabolism, we adopted the *gh3* octuple mutant, in which IAA inactivation via conjugation to amino acids is deficient[67]. The activity of enzymes from this family was recently shown to be the first step in auxin catabolism[68]. By measuring root growth after 6 days of treatment with IAA or 4-CPA at 10 nM (conditions showing similar effect on growth of Col-0 roots, Fig. 3a,g) we found the *gh3* plants to be hyper-sensitive to IAA, but not to 4-CPA (Fig. 3g). These results are in line with previous conjugation rates measured for 2,4-D vs. IAA[44], and favors the assumption that 4-CPA is not an efficient substrate for the main IAA-inactivation pathway in *Arabidopsis*. Collectively, this body of evidence suggests that 4-CPA weak binding to the auxin receptors is compensated by enhanced cellular persistence. Thus, the prolonged auxin signaling following **1q** application is achieved not only due to the slow release of 4-CPA, but also as a consequence of 4-CPA bypassing key auxin homeostasis regulators.

4-CPA release is enzymatically regulated in plants

The rapid de-esterification of **1q** in *E. grandis* implies that 4-CPA release rate is largely determined by its amide bond hydrolysis (Fig. 2c). To investigate the mechanism of this step, we synthesized 4-CPA conjugated to D-Trp-OMe, forming the enantiomer of **1q** (**1s**, Fig. 4a). Since enantiomers

possess similar chemical and physical properties, differences in their hydrolysis rate (or activity) *in planta* could be attributed to enzymatic regulation. HPLC-MS/MS analysis of apical and basal parts of *E. grandis* cuttings 24 h after application of **1q** or **1s** showed that 4-CPA accumulates only in response to **1q** treatment (Fig. 4a). Furthermore, in a root elongation assay using *Arabidopsis* seedlings, **1q** was found to engender ~100-fold stronger inhibitory response than **1s** (Supplementary Fig. 12). From these results, a major role for enzymatic cleavage in 4-CPA release can be inferred. Members of the metallopeptidases family; IAA-Leu-RESISTANT1 (ILR1)/ILR1-like (ILLs) are known to hydrolase amides of indole-based compounds[69–72], raising the possibility of a similar amido-hydrolase activity towards **1q** and/or **1r**. To test this hypothesis, we adopted the *Arabidopsis* triple mutant *ilr1 ill2 iar3*, which shows a compromised response to a range of IAA-amino acid conjugates[68,73]. The *ilr1 ill2 iar3* triple mutant was insensitive to **1q** in root elongation (continuous incubation, measured after 3 days, Fig. 4b) and in AR induction in etiolated seedlings (brief shoot application, Fig. 4c, Supplementary Fig. 13) assays. To validate these results, the appropriate GST-recombinant *Arabidopsis* enzymes were tested *in vitro* for their activity against **1q** and **1r**, or against IAA-alanine (IAA-Ala), an established substrate[71] serving to verify the enzymes activity in the assay. While all three enzymes hydrolyzed IAA-Ala (Supplementary Fig. 14), only ILR1 and ILL2 efficiently hydrolyzed **1r**, and none hydrolyzed the parent **1q** (Fig. 4d). Of note, a marginal but detectable activity of ILR1 and ILL2 was also detected against the D-enantiomer of **1r** (**1t**, Supplementary Fig. 14d), which might explain the minor bioactivity observed for its parent compound **1s** in *Arabidopsis* (Supplementary Fig. 12). In an attempt to better understand their specificities, we turned to the three-dimensional structures of the three enzymes, using the available X-ray crystal structure of ILL2[74], and AlphaFold[75] predictions for ILR1 and IAR3. We found the ligand-binding pockets of the two active enzymes, ILR1 and ILL2, to contain a deep hydrophobic niche, in contrast to the pocket of IAR3, which is elongated, shallow and contains a smaller hydrophobic patch (Supplementary Fig. 15). In agreement, molecular docking calculations (Glide, Schrödinger, 2021-4) positioned the non-polar indole of **1r** inside the deep hydrophobic niche of the active enzymes, while in the non-active IAR3, neither the indole nor the phenoxy group formed sufficient non-polar interactions with the catalytic pocket (Fig. 4d). Further correlating the ligand-pocket non-polar interactions to substantial enzymatic activity, docking analysis positioned the indole group of IAA-Ala inside the IAR3 pocket, in close interaction with the hydrophobic patch (Supplementary Fig. 16). Having established that ILR1 and ILL2 are responsible for the hydrolysis of **1r**, we nevertheless observed a residual root growth inhibition for *ilr1 ill2 iar3* in response to longer incubation durations with **1q** (Supplementary Fig. 17), implying participation of additional amidohydrolase (Ah). We speculated that other ILL enzymes might underlie this effect, and

generated two quintuple mutant lines; *ilr1 ill2 iar3 ill3 ill5* and *ilr1 ill2 iar3 ill1 ill6* (termed quintuple *3,5* or *1,6* respectively) using CRISPR-Cas9 (Supplementary Fig. 18–21). The *quintuple 3,5* was only slightly less sensitive to a 7-days incubation with **1q** (0.5 M) compared to the triple mutant, while the *quintuple 1,6* was entirely resistant (Supplementary Fig. 17a). Structural modelling of the four enzymes (ILL1,3,5, and 6) revealed differences in the hydrophobicity and geometry of their ligand binding sites, with ILL1 and ILL6 binding sites being more hydrophobic than those of ILL3 and ILL5 (Supplementary Fig. 17b). Collectively, we established that the second, rate-limiting, step in 4-CPA release is enzymatically regulated, and that members of the ILR1/ILLs family are the major enzymes cleaving **1r** to release 4-CPA *in planta*.

Structural conservation of ILR1 ligand binding pocket contributes to 4-CPA release

Identifying specific members of the ILR1/ILLs family as the main activators of **1q** *in planta* opened the door to rationalizing and predicting its activation in other difficult-to-root cultivars. To this end, we performed a phylogenetic analysis based on 301 ILR1/ILLs proteins from 43 seed-plants (Extended Data - Tables 1 and 2) that suggested two sub-trees (Fig. 5a). The two super-families are composed of two (AhA1-A2) and three (AhB1-3) distinct groups, with members of *Arabidopsis* occupying the AhA1 (ILL3), AhA2 (ILR1), AhB1 (ILL6), and AhB2 (ILL1, ILL2, IAR3 and ILL5) groups (Fig. 5a). We first sought to determine if activation of **1q** is functionally conserved between *Arabidopsis* and *E. grandis*. The *E. grandis* genome contains 11 *ILR1/ILLs* genes, of which we suggest only 9 to be active; based on proteins sequence-length and transcriptome of manually enriched vascular-cambium tissue (Fig. 5b, Extended Data Table 1, Supplementary Fig. 22). We focused on family AhA2 due to its high-confidence topology compared to AhB2 (Fig. 5a and alternative tree in Supplementary Fig. 23), and since the single *E. grandis* protein in the AhB1 group is apparently a pseudogene (*Eucgr.F03795*; expression not detected, and short putative protein sequence of 290 amino acids, Fig. 5b and Extended Data, Table 1). Of the 3 active AhA2 genes, *EgK02589* (the suggested direct ortholog of ILR1; Fig. 5a) and *EgK02598* (which is clustered at the other orthologous group of Ah2A) were found to be highly expressed in vascular-cambium obtained 24 h after K-IBA treatment (Fig. 5b). The two genes were separately over-expressed in the *Arabidopsis ilr1 ill2 iar3* triple mutant background and their enzymatic activity was inferred from a root-growth complementation assay in the presence of **1q**. Interestingly, while lines overexpressing *EgK02589* restored the sensitivity to **1q** in a root-growth inhibition assay, lines expressing *EgK02598* did not (Fig. 5c). In agreement, structural modeling and docking calculations found the ligand binding pocket of EgK02598 flatter than those of EgK02589 and ILR1, and less

favorable for the indole or phenoxy groups of **1r** to form significant non-polar and van der Waals interactions (Fig. 5d). These observations promote the hypothesis that EgK02589 contributes to the hydrolysis of **1q** to release active 4-CPA in the cambium. To broaden this observation, we similarly tested the activity of orthologs of ILR1/EgK02589 from *Populus trichocarpa* (Potri.006G207400, Pt400) and *Prunus persica* (Prupe.7G100000, Pp000), and one ortholog of EgK02598 from *Populus trichocarpa* (Potri.016G074100, Pt100). Again, only Pt400 and Pp000 but not Pt100 restored the response to **1q** (Fig. 5c), a trend that was further supported by structural modeling and docking calculations (Fig. 5d).

Collectively, the above experiments provide evidences that structural conservation of the ligand binding pocket among members of the ILR orthologous group supports **1r** cleavage, demonstrating the potential of structural modeling and docking calculations to predict the activation of **1q** in various plant species.

1q enhances adventitious roots formation in a range of distantly related woody species

The experimental evidences for enhanced de-novo root regeneration following **1q** application, together with the conservation of its key activating enzymes in diverse plant species, inspired us to examine the utility of **1q** in alleviating the barrier to rooting of agriculturally and environmentally-important difficult-to-root cultivars. We first examined *Eucalyptus x trabutii*; a very difficult to propogate hybrid of *E. camaldulensis* and *E. botryoides*, that has a relatively high resistance to cold[76] and is important in supporting honeybee nutrition during the Israeli autumn[77]. For this hybrid, a combined application of **1q** and K-IBA dramatically outpreformed K-IBA alone in rooting efficency (45% vs. none, Fig. 6a). Likewise, for the apple (*Malus domestica*) rootstock clone CG41, which supports high yields, dwarfism and resistance to soil diseases but is considered difficult-to-root[78–80], supplementation of **1q** increased rooting rate by ~2-fold compared to K-IBA alone (Fig. 6b). As part of our efforts to support local cultivation of the argan tree (*Argania spinosa*); a species known for its tolerance to extreme environmental conditions and for its valuable oil, we evaluated several clones: three difficult-to-root clones (C124, C127, and ARS7[81]), of which the first two were directly obtained from the first trees that were planted in Israel as part of a botanical garden in 1931, and an easy-to-root clone, ARS1[81]. Application of **1q** doubled the rooting rates of cuttings from the >90-year-old C127 plant material but did not increase the low rooting efficiencies of C124 (Fig. 6c). For ARS7, again, **1q** doubled the basal root formation response to K-IBA, while for the more permissive ARS1, maximal response was found in both treatments (Fig. 6c). The success of the combined K-IBA + **1q** treatment enabled us to generate several plantations of selected elite clones of argan for further analyzing yield and profitability under different soil and climate conditions

around the country (Supplementary Fig. 24). Altogether, these results suggest that woody, mature cuttings, for which poor regeneration rates are attributed to low auxin sensitivity, the saturated effect of IBA can be increased by low levels of **1q** (M range). The results further suggest that ectopic addition of IBA is not necessarily a prerequisite for the rooting enhancement response to **1q** in mature woody tissues. Indeed, the rooting rates of *Populus alba* cuttings were doubled following application of **1q** as a standalone treatment (Fig. 6d). In line with the hypothesis of a conserved enzymatic hydrolysis being responsible for 4-CPA release, the basal parts of cuttings from *Eucalyptus x trabutii*, the ARS7 argan line, and *Populus alba* accumulated 4-CPA dominantly following **1q** application but not of its enantiomer **1s** (Supplementary Fig. 25).

Conclusion and outlook

A model of the dynamics and metabolic fate of **1q** *in planta* is presented in Figure 7a. We suggest that following application, **1q** efficiently penetrates into the plant tissues and then into cells due to its neutral charge at a physiological pH and overall hydrophobicity. In the cells, the ester bond is quickly hydrolyzed (either chemically or by abundant cellular esterases) forming **1r**, which is mostly ionized in the cellular pH and therefore trapped inside the cell in the absence of efficient active transport[82]. Alternatively, **1q** could be hydrolyzed extracellularly. This scenario, however, is less likely considering that the highly acidic **1r** (predicted pK_a 3.3) is mostly ionized in the apoplast pH, which will result in low cellular accessibility[82]. In agreement, in long-exposure root elongation assays that mitigate differences in the uptake of small molecules, *Arabidopsis* roots were found to be more sensitive to **1q** than to **1r** (Supplementary Fig. 12). Subsequently, **1r** is cleaved by members of the ILR1/ILLs family, which presumably reside in the endoplasmic reticulum and in the cytosol[70,83], to release 4-CPA intracellularly. Thus, although the measurements in *E. grandis* cutting bases detected comparable maxima levels of 4-CPA following **1q** or free 4-CPA treatments (Fig. 2c,d), we suggest higher intracellular accumulation of 4-CPA in response to **1q**. Practically, the dynamics and metabolic fate of **1q** *in planta* translate into a slow-release mechanism of a bioactive auxin inside the cells.

While the immediate auxin signaling elicited by 4-CPA is weaker than the one evoked in response to a native auxin, the higher cellular stability of 4-CPA supports an amplified and more sustained signaling over time. We provide biochemical evidence that 4-CPA is not a favorable substrate to the PIN8 transporter, and genetic evidence for its low affinity to the IAA conjugating enzymes GH3s[84]. Since transport and conjugation are two of the main feedback responses to auxin[85,86], we suggest that evading these homeostasis regulators further contributes to prolonged auxin signaling. We also

provide data suggesting that 4-CPA is able to move basipetally, and that AUX1 is required for its rooting enhancement effect. This in turn suggests that 4-CPA is a subject of an uncharacterized efflux transporter, which may support the compound basipetal movement, presumably through the phloem bulk flow, following apical application. Whether apical response to 4-CPA contributes indirectly to AR formation remains an open question. Identification of 4-CPA homeostasis regulators (e.g. metabolism, transport) will provide a better understanding of the contribution of these processes to the activity of **1q**. The delivery model we describe offers an advantage over the traditional application of free auxins (e.g., IBA, NAA, etc.) that are typically mostly ionized in the apoplast and may require active transport for efficient uptake. Together, our observations suggest that the short dual application of IBA and **1q** enables a fast and strong auxin response (K-IBA applied at mM concentrations) followed by a prolonged and sustaining signaling (**1q** applied at M) (Fig. 7b).

Using a two-phases of auxin treatment, Ludwig-Muller et al. were able to distinguish between induction of callus proliferation and AR establishment[54]. In analogy to our system, a higher-resolution understanding of how the two compounds interact (temporally and spatially) during AR induction and development is of significant mechanistic and practical interest, and may assist in optimizing future applications. Moreover, the flexible molecular design of a synthetic auxin conjugate can be further fine-tuned by modulating either the synthetic auxin or its conjugated amino acid to provide a palette of auxin responses varying in strength and duration that could be tailored to different plant species and even specific clones. Finally, the slow-release approach as applied herein can be incorporated into other agricultural practices in which auxin is applied beyond as herbicides, such as modulating root system complexity or the timing of fruits set, to allow for more optimized responses.

Acknowledgments

We thank the undergraduate students Ariel Verblun and Geffen Yehezkely in R.W. lab for supporting experiments. We also thank Eilon Shani for providing *DR5:Luciferase*, *DR5:Venus*, and *aux1-7 Arabidopsis* lines, Malcolm Bennett and Ranjan Swarup for providing the *aux/lax* quadruple mutant, Mark Estelle for providing Y2H vectors, Karin Ljung for providing the *gh3* octuple mutant, and Bonnie Bartel for providing the *ilr1-1 ill2-1 iar3-2* triple mutant and vectors expressing GST-recombinant version of ILR1, ILL2, and IAR3. We also thank Itay Mayrose and Keran Halabi for their assistance in constructing ILR1/ILLs phylogenetics. This work was supported by funding from the Israel Science Foundation (grant number 1057/21 to R.W.), the Chief Scientist of the Ministry of Agriculture and Rural Development, Israel (grant numbers 20-10-0067, 13-37-0005 and 20-01-0270 to R.W. and E.S.), the US-Israel Binational Agricultural Research and Development Fund (BARD, grant number IS-5195-19R to R.W, E.S, and Chris J. Staiger (Purdue University, IN)), and the Yuri Milner 70@70 Fellowship (to O.R.).

Data Availability

All data supporting the findings of this study are available within the paper and its Supplementary Information. For the RNA sequencing experiments, accession codes will be available before publication.

References

1. Verstraeten, I., Schotte, S. & Geelen, D. hypocotyl adventitious root organogenesis differs from lateral root development. *Front. Plant Sci.* **5**, (2014).

2. Hartmann, H. T., Kester, D. E., Davis, F. T., Geneve, R. L., Wilson, S. B., *Hartmann & Kester's Plant Propagation: Principles and Practices* (Pearson, 2017)

3. Poethig, R. S. Phase change and the regulation of shoot morphogenesis in plants. *Science (1979)* **250**, 923–930 (1990).

4. Pijut, P. M., Woeste, K. E. & Michler, C. H. Promotion of adventitious root formation of difficult-to-root hardwood tree species. *Hortic. Rev.* **38**, 213 (2011).

5. Hackett, W. P. Juvenility, maturation, and rejuvenation in woody plants. *Hortic. Rev.* **7**, 109–154 (2011).

6. Wilcox, J. R. & Farmer, R. E. Heritability and C effects in early root growth of eastern cottonwood cuttings. *Heredity* **23**, 239–245 (1968).

7. Grattapaglia, D., Bertolucci, F. L. & Sederoff, R. R. Genetic mapping of QTLs controlling vegetative propagation in *Eucalyptus grandis* and *E. urophylla* using a pseudo-testcross strategy and RAPD markers. *Theoretical and Applied Genetics* **90**, 933–947 (1995).

8. Visser, E. J. W., Cohen, J. D., Barendse, G. W. M., Blom, C. W. P. M. & Voesenek, L. A. C. J. An ethylene-mediated increase in sensitivity to auxin induces adventitious root formation in flooded Rumex palustris Sm. *Plant Physiol.* **112**, 1687–1692 (1996).

9. Sorin, C. *et al.* Auxin and light control of adventitious rooting in Arabidopsis require ARGONAUTE1. *Plant Cell* **17**, 1343–1359 (2005).

10. Bellini, C., Pacurar, D. I. & Perrone, I. Adventitious roots and lateral roots: similarities and differences. *Annu. Rev. Plant Biol.* **65**, 639–666 (2014).

11. Pacurar, D. I., Perrone, I. & Bellini, C. Auxin is a central player in the hormone cross-talks that control adventitious rooting. *Physiol. Plant.* **151**, 83–96 (2014).

12. Caboni, E. et al. Biochemical aspects of almond microcuttings related to in vitro rooting ability. *Biol. Plant.* **39**, 91–97 (1997).

13. Lakehal, A. et al. A molecular framework for the control of adventitious rooting by TIR1/AFB2-Aux/IAA-dependent auxin signaling in *Arabidopsis*. *Mol. Plant* **12**, 1499–1514 (2019).

14. Bellamine, J., Penel, C., Greppin, H. & Gaspar, T. Confirmation of the role of auxin and calcium in the late phases of adventitious root formation. *Plant Growth Regul.* **26**, 191–194 (1998).

15. Blažková, A. et al. Auxin metabolism and rooting in young and mature clones of *Sequoia sempervirens*. *Physiol. Plant.* **99**, 73–80 (1997).

16. Rasmussen, A., Hosseini, S. A., Hajirezaei, M.-R., Druege, U. & Geelen, D. Adventitious rooting declines with the vegetative to reproductive switch and involves a changed auxin homeostasis. *J. Exp. Bot.* **66**, 1437–1452 (2015).

17. Abu-Abied, M. et al. Microarray analysis revealed upregulation of nitrate reductase in juvenile cuttings of *Eucalyptus grandis*, which correlated with increased nitric oxide production and adventitious root formation. *Plant J.* **71**, 787–799 (2012).

18. Abarca, D. et al. The GRAS gene family in pine: transcript expression patterns associated with the maturation-related decline of competence to form adventitious roots. *BMC Plant Biol.* **14**, 354 (2014).

19. Fahn, A. *Plant Anatomy*. (Pergamon, 1990)

20. Uggla, C., Moritz, T., Sandberg, G. & Sundberg, B. Auxin as a positional signal in pattern formation in plants. *Proc. Natl. Acad. Sci. U.S.A* **93**, 9282–9286 (1996).

21. Tuominen, H., Puech, L., Fink, S. & Sundberg, B. A radial concentration gradient of indole-3-acetic acid is related to secondary xylem development in hybrid aspen. *Plant Physiol.* **115**, 577–585 (1997).

22. Ballester, A., SAN-JOSÉ, M. C., Vidal, N., Fernández-Lorenzo, J. L. & Vieitez, A. M. Anatomical and biochemical events during in vitro rooting of microcuttings from juvenile and mature phases of chestnut. *Ann. Bot.* **83**, 619–629 (1999).

23. Vidal, N., Arellano, G., San-José, M. C., Vieitez, A. M. & Ballester, A. Developmental stages during the rooting of in-vitro-cultured Quercus robur shoots from material of juvenile and mature origin. *Tree Physiol* **23**, 1247–1254 (2003).

24. Legué, V., Rigal, A. & Bhalerao, R. P. Adventitious root formation in tree species: involvement of transcription factors. *Physiol. Plant.* **151**, 192–198 (2014).

25. Ranjan, A. et al. Molecular basis of differential adventitious rooting competence in poplar genotypes. *J. Exp. Bot.* **73**, 4046–4064 (2022).

26. Díaz-Sala, C. Direct reprogramming of adult somatic cells toward adventitious root formation in forest tree species: the effect of the juvenile–adult transition. *Front. Plant Sci.* **5**, (2014).

27. Solé, A. et al. Characterization and expression of a Pinus radiata putative ortholog to the Arabidopsis SHORT-ROOT gene. *Tree Physiol.* **28**, 1629–1639 (2008).

28. Abu-Abied, M. et al. Gene expression profiling in juvenile and mature cuttings of *Eucalyptus grandis* reveals the importance of microtubule remodeling during adventitious root formation. *BMC Genom.* **15**, 826 (2014).

29. de Almeida, M. R. et al. Reference gene selection for quantitative reverse transcription-polymerase chain reaction normalization during in vitro adventitious rooting in *Eucalyptus globulus* Labill. *BMC Mol. Biol.* **11**, 73 (2010).

30. de Almeida, M. R. et al. Comparative transcriptional analysis provides new insights into the molecular basis of adventitious rooting recalcitrance in *Eucalyptus*. *Plant Sci.* **239**, 155–165 (2015).

31. Ruedell, C. M., de Almeida, M. R. & Fett-Neto, A. G. Concerted transcription of auxin and carbohydrate homeostasis-related genes underlies improved adventitious rooting of microcuttings derived from far-red treated *Eucalyptus globulus* Labill mother plants. *Plant Physiol. Biochem.* **97**, 11–19 (2015).

32. Cooper, W. C. Hormones in relation to root formation on stem cuttings. *Plant Physiol.* **10**, 789 (1935).

33. Oinam, G., Yeung, E., Kurepin, L., Haslam, T. & Lopez-Villalobos, A. Adventitious root formation in ornamental plants: I. General overview and recent successes. *Propag. Ornam. Plants* **11**, 78–90 (2011).

34. Epstein, E. & Ludwig-Müller, J. Indole-3-butyric acid in plants: occurrence, synthesis, metabolism and transport. *Physiol. Plant.* **88**, 382–389 (1993).

35. Strader, L. C. & Bartel, B. Transport and metabolism of the endogenous auxin precursor indole-3-butyric acid. *Mol. Plant* **4**, 477–486 (2011).

36. Wiesman, Z., Riov, J. & Epstein, E. Comparison of movement and metabolism of indole-3-acetic acid and indole-3-butyric acid in mung bean cuttings. *Physiol. Plant.* **74**, 556–560 (1988).

37. Felker, P. & Clark, P. R. Rooting of mesquite (*Prosopis*) cuttings. *J. Range Manag.* **34**, 466-468 (1981).

38. Van der Krieken, W. M. et al. Increased induction of adventitious rooting by slow release auxins and elicitors. In *Biology of Root Formation and Development*. 95-104 (Springer, 1997).

39. Mihaljevic, S. & Salopek-Sondi, B. Alanine conjugate of indole-3-butyric acid improves rooting of highbush blueberries. *Plant Soil Environ.* **58**, 236–241 (2012).

40. Haissig, B. E. Influence of aryl esters of indole-3-acetic and indole-3-butyric acids on adventitious root primordium initiation and development. *Physiol. Plant.* **47**, 29–33 (1979).

41. Pizarro, A. & Díaz-Sala, C. Cellular dynamics during maturation-related decline of adventitious root formation in forest tree species. *Physiol. Plant.* **165**, 73–80 (2019).

42. Vilasboa, J., da Costa, C. T. & Fett-Neto, A. G. Rooting of eucalypt cuttings as a problem-solving oriented model in plant biology. *Prog. Biophys. Mol. Biol.* **146**, 85–97 (2019).

43. Quareshy, M., Prusinska, J., Li, J. & Napier, R. A cheminformatics review of auxins as herbicides. *J. Exp. Bot.* **69**, 265–275 (2018).

44. Eyer, L. et al. 2,4-D and IAA amino acid conjugates show distinct metabolism in *Arabidopsis*. *PLoS One* **11**, e0159269 (2016).

45. Yang, Y., Hammes, U. Z., Taylor, C. G., Schachtman, D. P. & Nielsen, E. High-affinity auxin transport by the AUX1 influx carrier protein. *Curr. Biol.* **16**, 1123–1127 (2006).

46. Hoyerova, K. et al. Auxin molecular field maps define AUX1 selectivity: many auxin herbicides are not substrates. *New Phytol.* **217**, 1625–1639 (2018).

47. Calderón Villalobos, L. I. A. et al. A combinatorial TIR1/AFB–Aux/IAA co-receptor system for differential sensing of auxin. *Nat. Chem. Biol.* **8**, 477–485 (2012).

48. Lee, S. et al. Defining binding efficiency and specificity of auxins for SCFTIR1/AFB-Aux/IAA co-receptor complex formation. *ACS Chem. Biol.* **9**, 673–682 (2014).

49. Vain, T. et al. Selective auxin agonists induce specific AUX/IAA protein degradation to modulate plant development. *Proc. Natl. Acad. Sci. U.S.A* **116**, 6463–6472 (2019).

50. Pufky, J., Qiu, Y., Rao, M. v, Hurban, P. & Jones, A. M. The auxin-induced transcriptome for etiolated Arabidopsis seedlings using a structure/function approach. *Funct. Integr. Genom.* **3**, 135–143 (2003).

51. Delargy, J. A. & Wright, C. E. Root formation in cuttings of apple in relation to auxin application and to etiolation. *New Phytol.* **82**, 341–347 (1979).

52. Verstraeten, I., Beeckman, T. & Geelen, D. Adventitious root induction in *Arabidopsis thaliana* as a model for in vitro root organogenesis. in *Plant Organogenesis: Methods and Protocols* 159–175 (Springer, 2013)

53. Grossmann, K. Auxin herbicides: current status of mechanism and mode of action. *Pest Manag. Sci.* **66**, 113–120 (2010).

54. Ludwig-Müller, J., Vertocnik, A. & Town, C. D. Analysis of indole-3-butyric acid-induced adventitious root formation on Arabidopsis stem segments. *J. Exp. Bot.* **56**, 2095–2105 (2005).

55. Blythe, E. K., Sibley, J. L., Tilt, K. M. & Ruter, J. M. Methods of auxin application in cutting propagation: a review of 70 years of scientific discovery and commercial practice. *J. Environ. Hortic.* **25**, 166–185 (2007).

56. Riov, J. et al. Improved method for vegetative propagation of mature *Pinus halepensis* and its hybrids by cuttings. *Isr. J. Plant Sci.* **67**, 5–15 (2020).

57. Eliasson, L. & Areblad, K. Auxin effects on rooting in pea cuttings. *Physiol. Plant.* **61**, 293–297 (1984).

58. Wain, R. L., Wightman, F. & Russell, E. J. The growth-regulating activity of certain ω-substituted alkyl carboxylic acids in relation to their β-oxidation within the plant. *Proc. R. Soc. Lond. B: Biol. Sci.* **142**, 525–536 (1954).

59. Behrens Richard & Howard Morton L. Some factors influencing activity of 12 phenoxy acids on mesquite root inhibition. *Plant Physiol.* **38**, 165–170 (1963).

60. Zimmerman, P. W. Several chemical growth substances which cause initiation of roots and other responses in plants. *Contrib. Boyce Thompson Inst.* **7**, 209–229 (1935).

61. Katekar, G. F. Auxins: on the nature of the receptor site and molecular requirements for auxin activity. *Phytochemistry* **18**, 223–233 (1979).

62. Kepinski, S. & Leyser, O. The *Arabidopsis* F-box protein TIR1 is an auxin receptor. *Nature* **435**, 446–451 (2005).

63. Dharmasiri, N., Dharmasiri, S. & Estelle, M. The F-box protein TIR1 is an auxin receptor. *Nature* **435**, 441–445 (2005).

64. Xuan, W., Opdenacker, D., Vanneste, S. & Beeckman, T. Long-term in vivo imaging of luciferase-based reporter gene expression in Arabidopsis roots. in *Root Development* 177–190 (Springer, 2018).

65. Ung, K. L. et al. Structures and mechanism of the plant PIN-FORMED auxin transporter. *Nature* **609**, 605–610 (2022).

66. Bainbridge, K. et al. Auxin influx carriers stabilize phyllotactic patterning. *Genes. Dev.* **22**, 810–823 (2008).

67. Casanova-Sáez, R. et al. Inactivation of the entire Arabidopsis group II GH3s confers tolerance to salinity and water deficit. *New Phytol.* **235**, 263–275 (2022).

68. Hayashi, K. et al. The main oxidative inactivation pathway of the plant hormone auxin. *Nat. Commun.* **12**, 1–11 (2021).

69. Bartel, B. & Fink, G. R. ILR1, an amidohydrolase that releases active indole-3-acetic acid from conjugates. *Science (1979)* **268**, 1745–1748 (1995).

70. Davies, R. T., Goetz, D. H., Lasswell, J., Anderson, M. N. & Bartel, B. *IAR3* encodes an auxin conjugate hydrolase from Arabidopsis. *Plant Cell* **11**, 365–376 (1999).

71. LeClere, S., Tellez, R., Rampey, R. A., Matsuda, S. P. T. & Bartel, B. Characterization of a family of IAA-amino acid conjugate hydrolases from *Arabidopsis*. *J. Biol. Chem.* **277**, 20446–20452 (2002).

72. Campanella, J. J., Olajide, A. F., Magnus, V. & Ludwig-Muller, J. A novel auxin conjugate hydrolase from wheat with substrate specificity for longer side-chain auxin amide conjugates. *Plant Physiol.* **135**, 2230–2240 (2004).

73. Rampey, R. A. et al. A family of auxin-conjugate hydrolases that contributes to free indole-3-acetic acid levels during Arabidopsis germination. *Plant Physiol.* **135**, 978–988 (2004).

74. Bitto, E. et al. X-ray structure of ILL2, an auxin-conjugate amidohydrolase from *Arabidopsis thaliana*. *Proteins.* **74**, 61–71 (2009).

75. Jumper, J. et al. Highly accurate protein structure prediction with AlphaFold. *Nature* **596**, 583–589 (2021).

76. Valentini, R., Mugnozza, G. S., Giordano, E. & Kuzminsky, E. Influence of cold hardening on water relations of three *Eucalyptus* species. *Tree Physiol.* **6**, 1–10 (1990).

77. Eliyahu, A. et al. Vegetative propagation of elite Eucalyptus clones as food source for honeybees (*Apis mellifera*); adventitious roots versus callus formation. *Isr. J. Plant Sci.* **67**, 83–97 (2020).

78. Robinson, T. L. et al. Performance of Cornell-Geneva rootstocks across North America in multi-location NC-140 rootstock trials. in *Proceedings of the 1st International Symposium on Rootstocks for Deciduous Fruit Tree Species.* 241–245 (2004, ISHS).

79. Marini, R. P. et al. Performance of 'golden delicious' apple on 23 rootstocks at 12 locations: a five-year summary of the 2003 nc-140 dwarf rootstock trial. *J. Am. Pomol. Soc.* **63**, 115 (2009).

80. Marini, R. P. *et al.* Performance of 'Golden Delicious' apple on 23 rootstocks at eight locations: a ten-year summary of the 2003 NC-140 dwarf rootstock trial. *J. Am. Pomol. Soc.* **68**, 54–68 (2014).

81. Tzeela, P. et al. Comparing adventitious root-formation and graft-unification abilities in clones of *Argania spinosa*. *Front. Plant Sci.* **13**, (2022).

82. Ruberv, P. H. & Sheldrake, A. R. Effect of pH and surface charge on cell uptake of auxin. *Nat. New Biol*. **244**, 285–288 (1973).

83. Sanchez Carranza, A. P. et al. Hydrolases of the ILR1-like family of Arabidopsis thaliana modulate auxin response by regulating auxin homeostasis in the endoplasmic reticulum. *Sci. Rep.* **6**, 24212 (2016).

84. Staswick, P. E. et al. Characterization of an Arabidopsis enzyme family that conjugates amino acids to indole-3-acetic acid. *Plant Cell* **17**, 616–627 (2005).

85. Hagen, G. & Guilfoyle, T. Auxin-responsive gene expression: genes, promoters and regulatory factors. *Plant Mol. Biol.* **49**, 373–385 (2002).

86. Wabnik, K., Govaerts, W., Friml, J. & Kleine-Vehn, J. Feedback models for polarized auxin transport: an emerging trend. *Mol BioSyst.* **7**, 2352–2359 (2011).

87. Kessel, A. & Ben-Tal, N. Free energy determinants of peptide association with lipid bilayers. *Curr. Top. Membr.* **52**, 205–253 (2002).

Manuscript Figures

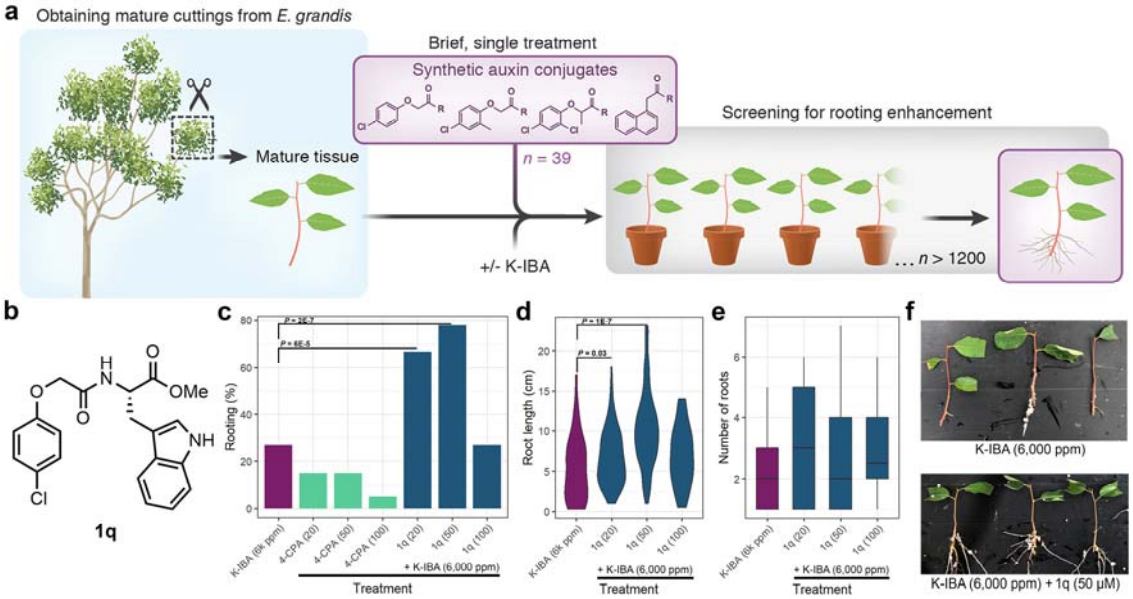

Fig. 1: A chemical screen for rooting enhancers of difficult-to-root cuttings highlighted 4-CPA-Trp-OMe (1q). a, Illustration of the chemical screen. **b**, structure of **1q**; the most efficient compound. **c**, Rooting percentages 1 month after application. Fisher's exact test p-values are presented for significantly better applications compared to K-IBA (6,000 ppm) as a single treatment. n = 60, 20, 20, 20, 45, 45, and 45 cuttings per sample, respectively. Compound concentration (in µM) is shown in brackets. **d**, Distributions of root-length in regenerated cuttings. Two-sided Mann-Whitney U test p-values are presented. **e**, Box-plot (center line, median; box limits, upper and lower quartiles; whiskers, 1.5x interquartile range) presenting number of roots per regenerated cutting. None of the applications outperformed K-IBA significantly (Mann-Whitney U test). **f**, Representative pictures of cuttings 35 days from the indicated treatment.

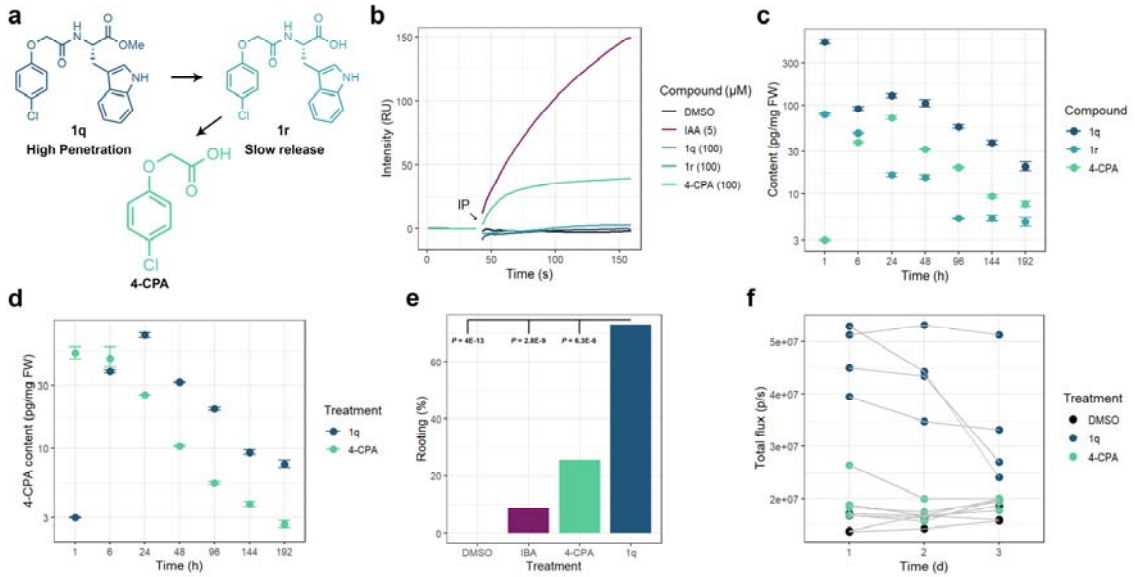

Fig. 2: 1q combines high penetration with slow 4-CPA release to facilitate prolonged auxin signaling. a, Schematic representation of 4-CPA release from **1q** *in planta*. **b**, SPR assay testing the intrinsic activity of the indicated compounds or DMSO (1%) *in-vitro* using TIR1 and IAA7 degron. IP stands for injection point of TIR1 mixed with the tested auxin in solution, RU stands for resonance unit. **c**, HPLC-MS/MS quantification of the compounds shown in **a** following application of **1q** (100 µM) + K-IBA (6,000 ppm). Each sample is composed of 3 replicates, extracted from a pool of 20 cutting-bases harvested together. Data presented in logarithmic scale. Error-bars represent standard errors. **d**, HPLC-MS/MS quantification of 4-CPA following **1q** (100 µM) + K-IBA (6,000 ppm) or 4-CPA (100 µM) + K-IBA (6,000 ppm). Each sample consists of 3 replicates except for 4-CPA after 1 h which consists of 2. Samples composition is as specified in **c**. Data presented in logarithmic scale. Error-bars represent standard errors. **e,** Percentages of two-week-seedlings (*Arabidopsis*) that developed adventitious roots in response to the indicated treatments (10 µM for IBA, 4-CPA or **1q**, and 0.1% for DMSO applied specifically to shoots for 1.5 h via a split-dish). Shown are p-values of Fisher's exact test testing the hypothesis that **1q** treatment results with higher rooting percentages. n = 37 ,35, 38, and 37 respectively. Averaged AR number for rooted seedlings treated with **1q** was 4.48±0.65 (SE), n = 27. f, Time-lapse quantification of *DR5:luciferase* activity in *Arabidopsis* seedlings following the indicated treatments (10 µM for 4-CPA or **1q**, 0.1% for DMSO. Shoot specific 1.5 h application). Each dot represents ~20 seedlings (pooled). *P* = 2.93E-05, repeated measures ANOVA.

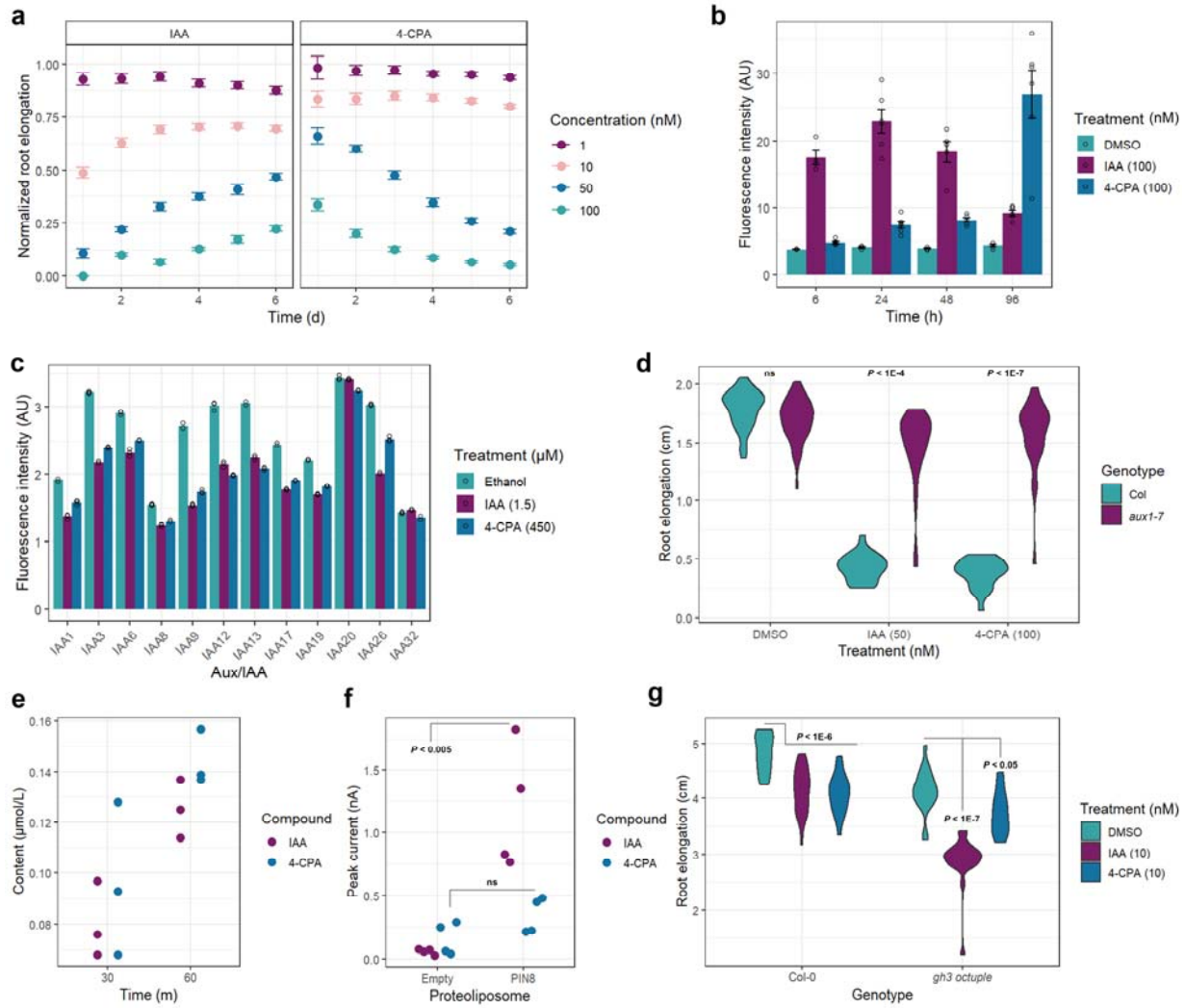

Fig. 3: Bypassing key auxin homeostasis regulators supports 4-CPA long-term signaling. a, Normalized root elongation of seedlings incubated with IAA or 4-CPA at the indicated concentrations (0.1% DMSO as control), n = 18–23 plants per sample. **b**, Activity of the auxin reporter *DR5:Venus* in roots. n = 4–6 root tips per sample. **c**, Quantitative Y2H assay using TIR1 and YFP-tagged Aux/IAAs and the indicated auxin or ethanol (0.1%) as mock. n = 3. **d**, Root elongation of *aux1-7* seedlings in response to 3 days treatment. n > 40 for auxins, n > 20 for DMSO (0.1%). Tukey HSD p-values are presented, ns stands for not significant. **e**, HPLC-MS/MS quantification of the indicated auxin in oocyte cells expressing AUX1 transporter. n = 3. **f**, Solid-supported membrane (SSM)-based electrophysiology assay with empty or PIN8-containing proteoliposomes, n = 4. Two-sided Student's t test p-values are presented. **g**, Root elongation of *gh3* octuple mutant plants in response to a 3-days treatment with the indicated compounds. n = 18–24 plants per sample. Tukey HSD p-values are presented. In all panels error-bars represent standard errors.

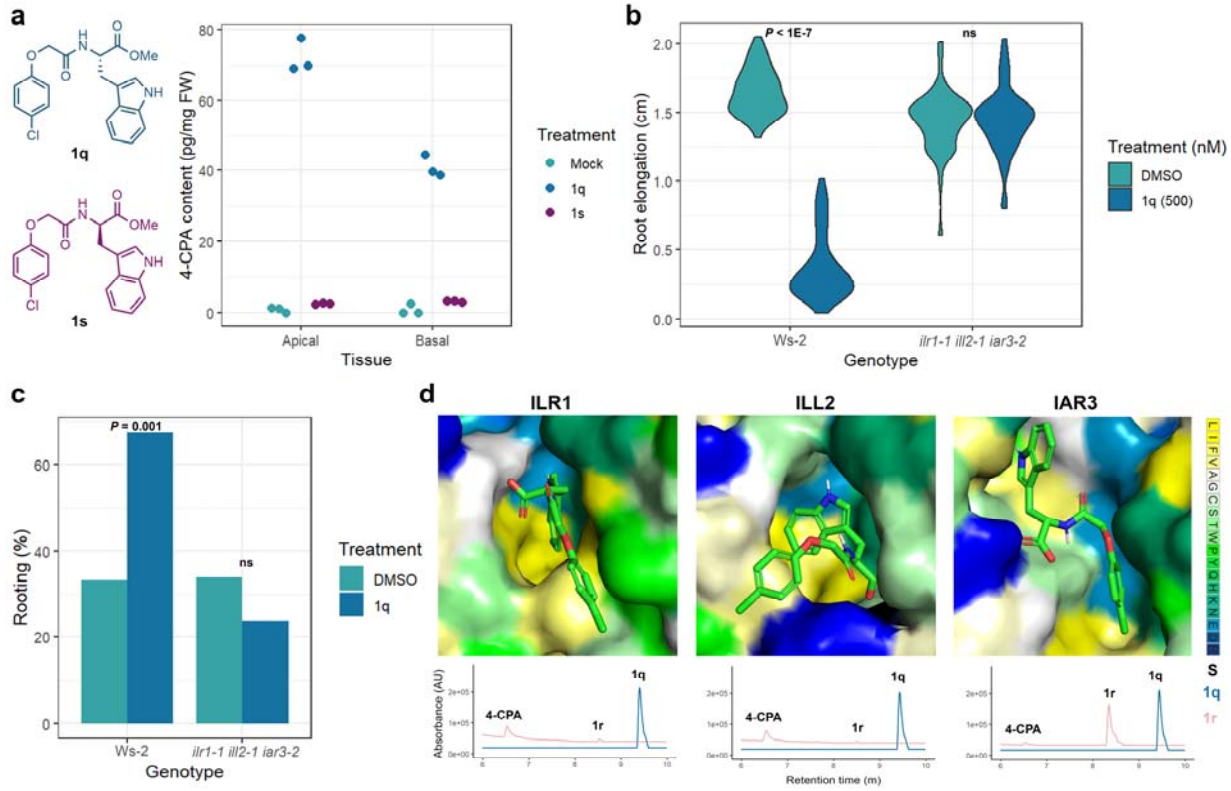

Fig. 4: 1r hydrolysis to 4-CPA is enzymatically regulated in *E. grandis* and *Arabidopsis*. **a**, Structures of the enantiomers **1q** and **1s** (*left*) and HPLC-MS/MS quantification of 4-CPA 24 h after apical or basal application with the indicated enantiomer (100 µM) + K-IBA basal treatment (6,000 ppm), or K-IBA (6,000 ppm) as mock (*right*). **b**, Root elongation of *ilr1-1 ill2-1 iar3-2* triple mutant in response to a 3-days treatment with **1q** or DMSO (0.1%). n = 47–54 plants per sample. Tukey HSD p-values are presented, ns stands for not significant. **c**, Percentages of seedlings developed adventitious roots in response to **1q** treatment (10 µM for **1q**, 0.1% for DMSO. Shoot specific 1.5 h application in a split-dish), n = 43–59 plants per sample. P-value of Fisher's exact test testing the hypothesis that **1q** treatment results with higher rooting percentages is shown. ns stands for not significant. **d**, *Top:* Docking calculations of **1r** with ILR1, ILL2 and IAR3. Amino acids are color-coded according to the Kessel/Ben-Tal hydrophobicity scale[87] (ranging from most hydrophobic (yellow) to most hydrophilic (blue)). *Bottom: In-vitro* hydrolytic activity of the enzymes towards **1q** (blue) or **1r** (pink) as monitored by HPLC-MS/MS. **1q** is not cleaved by any of the enzymes while **1r** is cleaved by ILR1 and ILL2 (but not IAR3) to release free 4-CPA.

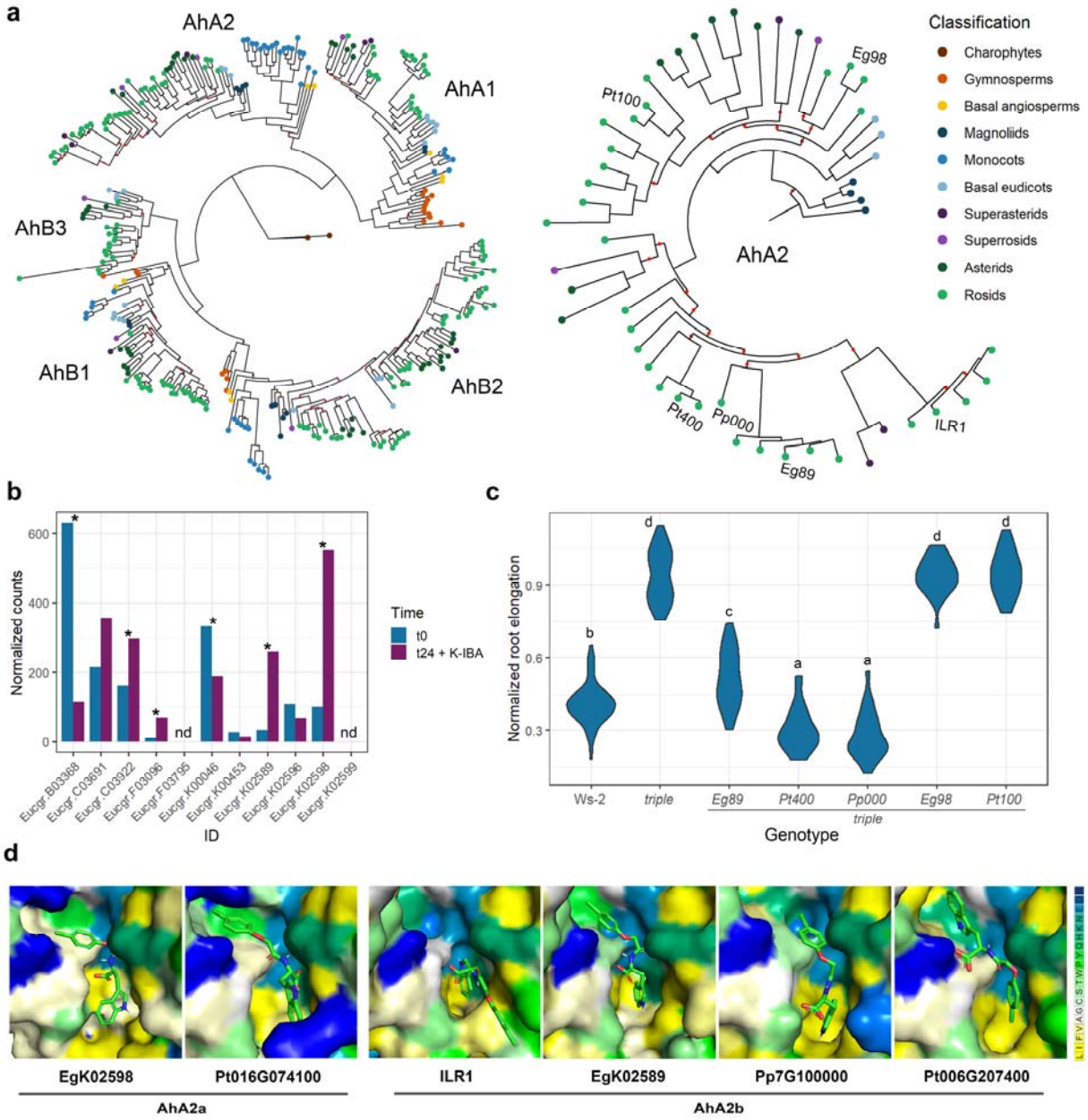

Fig. 5: Structural conservation of ILR1 ligand binding pocket contributes to 4-CPA release. a, *Left:* Phylogenetic analysis of ILR1/ILLs family in seed-plants. Sequences from the charophyte algae *Klebsormidium nitens* were used as an outgroup. *Right:* Sub-tree presenting the phylogeny of core angiosperm-sequences in family AhA2. Annotated are the characterized enzymes; EgK02598 (Eg98), Potri.016G074100 (Pt100), Potri.006G207400 (Pt400), Prupe.7G100000 (Pp000), EgK02589 (Eg89), and ILR1. Branches are annotated in brown or red for bootstrap values lower than 85 or 70, respectively. **b**, Expression profile (shown as normalized counts according to DESeq2) of *E. grandis* ILR1/ILLs in samples enriched for cambium tissue of mature cuttings, either immediately after collecting the tissue(t0; blue) or 24 h after K-IBA (6,000 ppm) submergence (t24 K-IBA; pink). Asterisks are indicators for significant differential expression according to DESeq2 ($P < 0.01$). nd stands for not detected. **c**, Normalized root elongation in response to 4-days treatment with **1q** (300 nM) or DMSO (0.1%) as mock. n = 78 or 72 for Ws-2 or *ilr1-1 ill2-1 iar3-2* (*triple*),

respectively, and 25–45 for over-expression lines. At least 10 T_2 lines for each transgene were characterized, and data was collected from single, homozygous lines. Lower-case letters indicate significant groups based on Tukey HSD test. **d**, Docking modeling of **1r** with the indicated enzymes. Amino acids are color-coded according to residues hydrophobicity raging from most hydrophobic (yellow) to most hydrophilic (blue)).

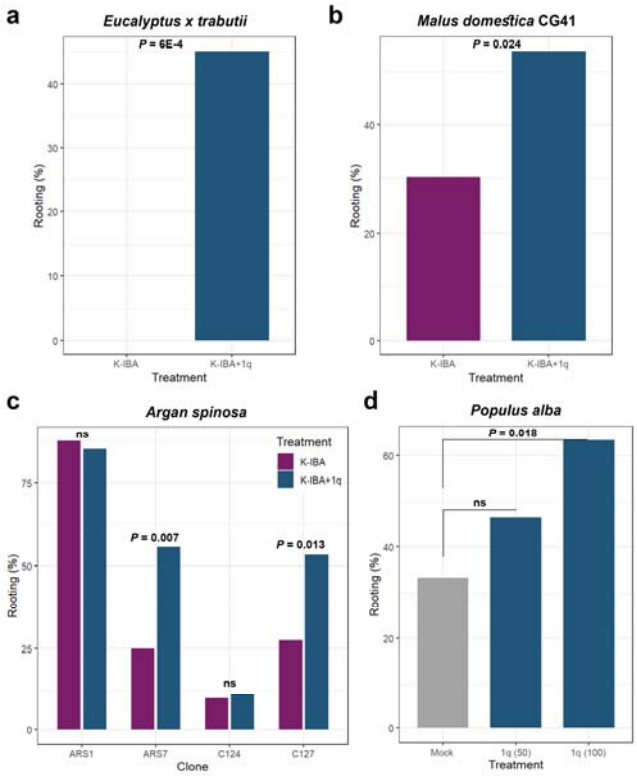

Fig. 6: 1q is a robust rooting enhancer for woody cuttings. a–c, Rooting percentages of mature cuttings obtained from the indicated species and clones applied with dual treatment of K-IBA (6,000 ppm) + **1q** (50 µM). n = 20 (**a**), 41 and 43 (**b**), 36–133 (**c**) cuttings per sample. P-values of Fisher's exact test testing the hypothesis that the dual treatment results with higher rooting percentages compare to K-IBA alone are shown. ns stands for not significant. **d**, Rooting percentages of mature cuttings obtained from *Populus alba* treated with **1q** as a single agent at the indicated concentrations (shown in brackets as µM). n = 30 cuttings per sample. P-value of Fisher's exact test testing the hypothesis that the **1q** treatment results with higher rooting percentages compare to mock (0.1% DMSO) is shown. ns stands for not significant. The duration of all experiments was 1–2 months.

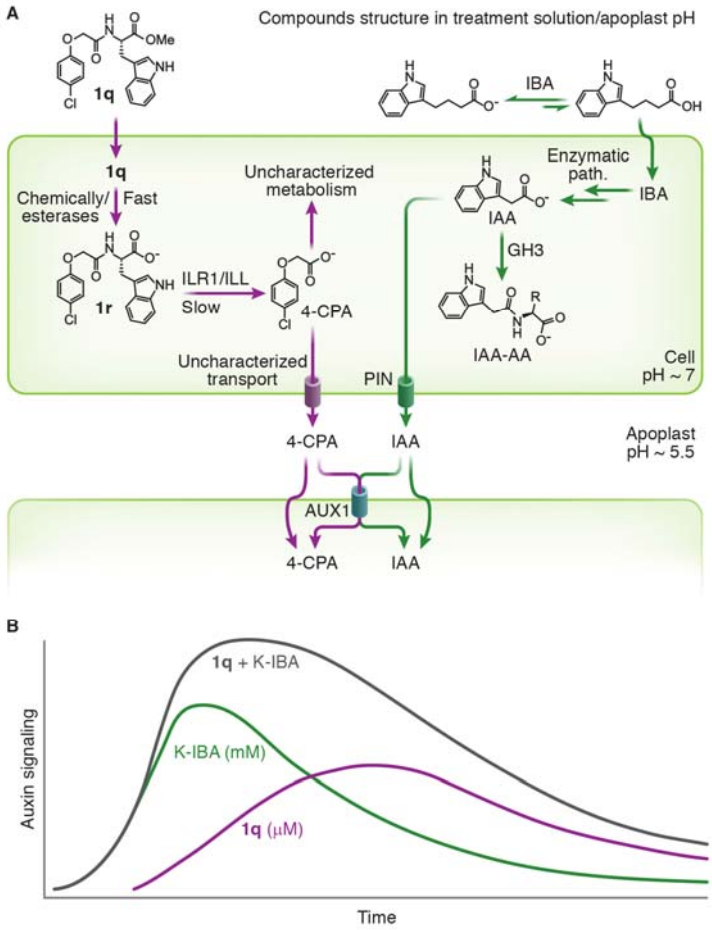

Fig. 7: Model comparing the fate of 1q and K-IBA following their application to woody cuttings. Schematic illustration of **1q** (purple) and K-IBA (green) fate when applied to woody cuttings (**a**) and their ensuing auxin signaling (**b**). Although K-IBA is applied at a very high concentration, its mostly negative charge under physiological conditions limits its accessibility to the plant, and later to cells. Inside the cell, IBA is converted into IAA, a strong yet highly regulated auxin. We suggest that these are the main factors underlying the auxin signaling pattern following a short K-IBA treatment (**b**). In contrast, **1q** is hydrophobic, limiting its concentration in a water-based solution, yet enabling enhanced tissue and cellular uptake. We suggest that efficient auxin delivery by **1q** is also a result of two distinct hydrolytic steps, responsible for a graduate, slow 4-CPA release. Moreover, 4-CPA is largely resistant to auxin feedback regulation, such as conjugation and transport, thus facilitating prolonged auxin signaling compared to IAA (**b**).